A NONLINEAR CIRCUIT MODEL FOR IMPATT DIODES

by

J. W. Gannett and L. O. Chua

Memorandum No. UCB/ERL M77/59

2 September 1977

ELECTRONICS RESEARCH LABORATORY

College of Engineering
University of California, Berkeley
94720

A NONLINEAR CIRCUIT MODEL FOR IMPATT DIODES[†]

J. W. Gannett and L. O. Chua[††]

ABSTRACT

An improved nonlinear circuit model for IMPATT diodes is presented for which each element bears a simple relationship with the physical operating mechanisms inside the device. The model contains lumped nonlinear elements as well as lumped and distributed linear elements. In its most general form it incorporates various second-order effects heretofore neglected in other circuit models. These include the effects due to unequal hole and electron ionization rates, unequal hole and electron drift velocities, and carrier diffusion.

[†]Research sponsored by the Office of Naval Research Contract N00014-76-0572 and by the Miller Institute which supported the second author during the 1976-77 Academic Year as a Miller Research Professor.

[††]Department of Electrical Engineering and Computer Sciences and the Electronics Research Laboratory, University of California, Berkeley, California 94720.

I. INTRODUCTION

The purpose of this paper is to present a nonlinear circuit model for IMPATT diodes (an acronym for IMPact Avalance Transit-Time). These semiconductor devices exhibit dynamic negative resistance at microwave frequencies. IMPATT diodes are utilized in microwave oscillators and amplifiers.

The circuit model for a given device has several uses. It is primarily an aid in designing and analyzing networks containing the device. An accurate circuit model would lead to realistic computer simulation of prototype circuit designs, thereby obviating or minimizing the need for carrying out expensive breadboarding analysis in the laboratory. Also, a good circuit model can offer insight into the device's operating mechanism. Such a model can serve as a useful tool in device design. The nonlinear circuit model presented in this paper is an improvement over those given previously in the literature [1,2,3] since each element in our basic model corresponds in a natural fashion to some physical operating mechanism inside the device. Furthermore, our model includes second-order effects heretofore neglected in other circuit models. These include effects due to unequal hole and electron ionization rates, unequal hole and electron drift velocities, and carrier diffusion.

Our circuit model contains linear and nonlinear lumped elements, as well as linear distributed elements. The avalanche region model is based on the analysis of Kuvås and Lee [4,5,6,7], which can be viewed as a more exact version of Read's [8] original analysis. It is composed entirely of lumped elements and contains the only nonlinearities in the model. The drift region is modeled with linear lumped and distributed elements. Under additional assumptions, our model reduces to one which is mathematically similar to those given previously [1,2,3]. However, there are differences which occur because our model is based on a more exact analysis.

Outlining the paper, in Section II we describe our general circuit model. We derive the quantitative aspects of this model in Sections III and IV. The evaluation of the model parameters is discussed in Section V. After making some simplifying assumptions, we obtain a first-order circuit model which is presented in Section VI.

II. THE GENERAL CIRCUIT MODEL

In this section we present our general circuit model and describe the physical significance of each of its basic elements.

To analyze the IMPATT diode, we divide its active portion into two regions.

There is a narrow "avalanche region" where the electric field is strong enough to cause carrier multiplication by impact ionization. Adjacent to the avalanche region, on one or both sides, is a longer "drift region."

The circuit model given in this section is based on the following assumptions: (a) the diode has a uniform cross-sectional area and can be treated as a one-dimensional device; (b) the time variations of the physical variables are "slow" compared to the carrier transit time in the avalanche region; (c) recombination and thermal generation of carriers is negligible; (d) the carriers travel at saturated velocities; and (e) the diffusion constants are not functions of any physical variables such as the electric field.

At this point, it is appropriate to define our notation. We use p and n for the hole and electron densities, respectively. The other symbols we use are listed in Table I. We attach the subscript p or n to D, v, or α to denote the corresponding quantity for holes or electrons, respectively.

In Fig. 1 the general circuit model of a single-drift region (SDR) IMPATT diode is shown. A partial derivation of the model is given in Appendix A; other details are given in Sections III and IV. This paper will deal only with the SDR diode, but as we shall see our model can be extended easily to the double-drift region (DDR) diode.

We shall begin our description of the model by considering the avalanche region. Assumption (b) is a key assumption which allows us to use a quasistatic approximation to obtain a nonlinear ordinary differential equation relating I_a to V_a. The derivation of this equation is the subject of Section III. Thus our model of the avalanche region consists of two basic elements. There is a lumped, dynamic, nonlinear one-port $\mathcal{N}$ through which the particle current I_a flows. In parallel with $\mathcal{N}$ is a linear capacitor C_a through which the displacement current flows. C_a is simply the geometrical capacitance of the avalanche region.

Figure 2(a) shows how the nonlinear one-port $\mathcal{N}$ can be modeled for simulation on a computer circuit analysis program. The circuit utilizes a linear inductor and a nonlinear controlled voltage source. In Fig. 2(b) we have shown how the equations can be rewritten so that a nonlinear inductor appears in place of the linear inductor. The constants b and ϕ_0 associated with the nonlinear inductor are arbitrary since they always drop out in the final network equations. Hence for convenience, we can choose b=1 and ϕ_0=0. However, if we choose

$$b = -\frac{d}{dV_a}\left(\frac{1}{M(V_a)\kappa(V_a)\tau(V_a)}\right)\Bigg|_{V_a=0} ,$$

then for moderate signal amplitudes it turns out that the voltage across the nonlinear controlled voltage source is relatively small. Thus, we can prove the often made intuitive statement that to a first-order approximation, the particle current in the avalanche region behaves as though it were flowing through a nonlinear inductor.

The drift region is modeled as the parallel combination of a linear capacitor C_d and a controlled current source I_e. The displacement current can be viewed as flowing through capacitor C_d, which is simply the geometrical capacitance of the drift region. Also, with the drift region extending from x=0 to x=W_d, the definition of I_e is (see (A-4))

$$I_e(t) \triangleq \frac{1}{W_d}\int_0^{W_d} I_d(x,t)\, dx. \tag{1}$$

It is evident that I_e is simply the spatial average of the particle current in the drift region. By assumption (b), the particle current injected into the drift region is approximately I_a. Thus, under the listed assumptions it turns out that I_e is the convolution of $I_a(\cdot)$ with a function $h(\cdot)$ which is given by

$$h(\lambda) \triangleq 0 \ , \ \lambda \leq 0 \ , \tag{2a}$$

$$\triangleq \frac{1}{2}\left[\operatorname{erf}\left(\frac{W_d - v\lambda}{2\sqrt{D\lambda}}\right) + \operatorname{erf}\left(\frac{v}{2\sqrt{D}}\sqrt{\lambda}\right)\right]$$

$$+ \frac{1}{v}\sqrt{\frac{D}{\pi\lambda}}\left[\exp\left(\frac{-v^2}{4D}\lambda\right) - \exp\left(\frac{-(W_d - v\lambda)^2}{4D\lambda}\right)\right], \quad \lambda > 0 \ . \tag{2b}$$

This is shown in Section IV. Hence, if we can synthesize a linear, distributed one-port with a current impulse response $h(\cdot)$, then we can model the drift region as shown in Fig. 3.

At this point it is appropriate to note that a DDR diode can be modeled by simply adding the equivalent circuit of the second drift region in series.

The constant sources I_0 and V_0 are the terminal current and voltage, respectively, under static conditions. I_0 is simply the value of the bias current

when the bias is derived from a constant current source, which is the usual case. Note that the parameter V_0 does not affect the RF performance of the device.

Finally, we remark that our model is valid only when the total terminal current I is positive.

III. DETAILS OF THE AVALANCHE REGION MODEL

In this section we discuss the differential equation for the nonlinear one-port $\mathcal{N}$ associated with the avalanche region model (see Fig. 1). The results given here are based on the work of Kuvås [4]. Most of the results in [4] were published in three papers by Kuvås and Lee [5,6,7].

The derivation of the differential equation for $\mathcal{N}$ is lengthy and is given in Appendix B. There it is shown to have the following form (see (A-39)):

$$\frac{dI_a}{dt} + \frac{I_a(t)+I_0}{M(V_a)\kappa(V_a)\tau(V_a)} = \frac{I_s}{\kappa(V_a)\tau(V_a)} + \eta(V_a)\left[I_a(t)+I_0-\rho(V_a)I_s\right]\frac{dV_a}{dt} \qquad (3)$$

where $M(\cdot)$, $\kappa(\cdot)$, $\tau(\cdot)$, $\eta(\cdot)$, and $\rho(\cdot)$ are nonlinear functions of V_a. To obtain these functions it is necessary to know the doping profile in the avalanche region. The procedure for calculating these functions is given in Appendix B, and in general they must be evaluated numerically.

We shall now consider the special case of a PIN doping profile at low current density. Most analyses are based on this assumption, and it is important here because closed-form expressions can be obtained for the nonlinear functions appearing in (3). In this case, the electric field used in evaluating the ionization integrals is independent of the spatial variable x and is given by

$$E^0(t) = E_c + E_a(t) = E_c + V_a(t)/W \qquad (4)$$

where W is the width of the high-field intrinsic region (compare (A-30)). With the electric field independent of x, it turns out that

$$\rho(V_a) \equiv 1 \qquad (5)$$

and the expressions for $(\tau)^{-1}$ and $(M\tau)^{-1}$ are

$$\frac{1}{\tau} = \frac{z(v_n+v_p)}{1+r}\left(\frac{1+re^{zW}}{e^{zW}-1}\right) \tag{6}$$

$$\frac{1}{M\tau} = \frac{(v_n+v_p)\left(\alpha_n-\alpha_p e^{zW}\right)}{e^{zW}-1} \tag{7}$$

where

$$r \triangleq I_{ns}/I_{ps} \tag{8}$$

$$z \triangleq \alpha_n - \alpha_p \ . \tag{9}$$

In the limit as $z \to 0$, which corresponds to the low-field limit or the case of equal ionization rates, $(\tau)^{-1}$ becomes

$$\lim_{z\to 0}\frac{1}{\tau} = \frac{v_n+v_p}{W} \ . \tag{10}$$

Using (7) and (10), it can be seen that for the case of equal ionization rates,

$$\left.\frac{1}{M}\right|_{\alpha_n=\alpha_p=\alpha} = 1 - W\alpha. \tag{11}$$

The expressions for κ and η in the PIN case can be obtained by straightforward but tedious calculations using the equations given in Appendix B. The resulting expressions are lengthy, and we shall take the liberty of correcting any errors we have found in the work of Kuvås [4]. Our results are as follows. We divide κ into two terms,

$$\kappa = \kappa_{dr} + \kappa_{diff} \ , \tag{12}$$

where

$$\kappa_{dr} \triangleq 1 + \left[\frac{\frac{1}{v_p}+\frac{1}{v_n}e^{-zW}}{\left(1-e^{-zW}\right)^2}\right]\left[\left(\alpha_n v_p+\alpha_p v_n\right)\left(W-\frac{1-e^{-zW}}{z}\right) - v_p Wz\right]$$

$$+\frac{e^{-zW}}{\left(1-e^{-zW}\right)^2}\left(\frac{1}{v_n}+\frac{1}{v_p}\right)\left[W\left(\alpha_n v_p+\alpha_p v_n\right) - \left(v_n+v_p\right)\right]$$

$$+\left[\frac{v_p z}{1-e^{-zW}} + \frac{v_n z e^{-zW}}{1-e^{-zW}} - \left(\alpha_n v_p + \alpha_p v_n\right)\right]\left[\frac{\left(\frac{1}{v_n} + \frac{1}{v_p}\right)}{1-e^{-zW}}\left(\frac{W}{2} + \frac{1-e^{-zW}}{Wz^2}\right) - \frac{W}{2v_n}\right] \quad (13)$$

and

$$\kappa_{diff} = \frac{z}{1-e^{-zW}}\left\{\frac{-\frac{v_n}{D_n}}{\left(1-e^{-zW}\right)\left(z-\frac{v_n}{D_n}\right)^2}\left[e^{-zW} - \exp\left(-\frac{v_n}{D_n}W\right) + \frac{D_n}{v_n}\left(z-\frac{v_n}{D_n}\right)\left(1-\exp\left(-\frac{v_n}{D_n}W\right)\right)\right]\right.$$

$$+\frac{1-\exp\left(-\left(z+\frac{v_p}{D_p}\right)W\right)}{z+\frac{v_p}{D_p}} + \frac{1}{1-e^{-zW}}\left(\frac{\frac{v_n}{D_n}}{z-\frac{v_n}{D_n}} + \frac{\frac{v_p}{D_p}}{z+\frac{v_p}{D_p}}\right)\left(\frac{1-e^{-zW}}{z} - We^{-zW}\right)$$

$$\left.+\frac{\frac{v_p}{D_p}e^{-zW}}{\left(1-e^{-zW}\right)\left(z+\frac{v_p}{D_p}\right)^2}\left[1-\exp\left(-\left(z+\frac{v_p}{D_p}\right)W\right) - \frac{D_p}{v_p}\left(z+\frac{v_p}{D_p}\right)\left(1-\exp\left(-\frac{v_p}{D_p}W\right)\right)\right]\right\}$$

$$+\frac{z}{1-e^{-zW}}\left\{\frac{D_p}{v_p^2} + \frac{1}{\left(1-e^{-zW}\right)\left(z+\frac{v_p}{D_p}\right)}\left[\frac{1}{v_p}e^{-zW} - \left(\frac{D_p}{v_p^2}\right)\left(z+\frac{v_p}{D_p}\right)\right]\right\}$$

$$\cdot\left\{\frac{\left(\alpha_n v_p + \alpha_p v_n\right)}{z+\frac{v_p}{D_p}}\left[1-\exp\left(-\left(z+\frac{v_p}{D_p}\right)W\right)\right] - \left[v_p + v_n\exp\left(-\left(z+\frac{v_p}{D_p}\right)W\right)\right]\right\}$$

$$+\frac{zw^{-zW}}{\left(1-e^{-zW}\right)^2}\left(\frac{\frac{1}{v_p}}{z+\frac{v_p}{D_p}} + \frac{\frac{1}{v_n}}{z-\frac{v_n}{D_n}}\right)\left[v_n + v_p - W\left(\alpha_n v_p + \alpha_p v_n\right)\right] + \frac{z}{\left(1-e^{-zW}\right)^2\left(z-\frac{v_n}{D_n}\right)}\left[\frac{1}{v_n} + \frac{D_n}{v_n^2}\left(z-\frac{v_n}{D_n}\right)\right]$$

$$\cdot\left\{\frac{\left(\alpha_n v_p + \alpha_p v_n\right)}{z-\frac{v_n}{D_n}}\left[\exp\left(-\frac{v_n}{D_n}W\right) - e^{-zW}\right] - \left[v_n e^{-zW} + v_p\exp\left(-\frac{v_n}{D_n}W\right)\right]\right\}$$

$$+\left[\frac{v_n z w^{-zW}}{1-e^{-zW}} + \frac{v_p z}{1-e^{-zW}} - \left(\alpha_n v_p + \alpha_p v_n\right)\right]\left\{\frac{D_p^2}{v_p^3 W}\left(1-\exp\left(-\frac{v_p}{D_p}W\right)\right)\right.$$

$$+\frac{1}{1-e^{-zW}}\left[\frac{\frac{D_n}{v_n^2W}}{\left(z-\frac{v_n}{D_n}\right)}\left(e^{-zW}-\exp\left(-\frac{v_n}{D_n}W\right)\right)+\frac{D_n^2}{v_n^3W}\left(1-\exp\left(-\frac{v_n}{D_n}W\right)\right)+\left(\frac{D_n}{v_n^2W}-\frac{D_p}{v_p^2W}\right)\left(\frac{1-e^{-zW}}{z}\right)\right.$$

$$\left.+\frac{\frac{D_p}{v_p^2W}}{z+\frac{v_p}{D_p}}\left(1-\exp\left(-\left(z+\frac{v_p}{D_p}\right)W\right)\right)-\frac{D_p^2}{v_p^3W}\left(1-\exp\left(-\frac{v_p}{D_p}W\right)\right)\right]\Bigg\}. \qquad (14)$$

The significance of κ_{diff} is that it goes to zero in the absence of diffusion. In the limit as $z \to 0$, which corresponds to the low-field limit or the case of equal ionization rates, the above expressions reduce to

$$\lim_{z\to 0}\kappa_{dr}=\frac{(v_p+v_n)^2}{6v_pv_n} \qquad (15)$$

$$\lim_{z\to 0}\kappa_{diff}=\frac{v_n+v_p}{v_n}\left(\frac{D_n}{v_nW}\right)\left\{\frac{1}{2}+\left(\frac{D_n}{v_nW}\right)^2\left[\left(1+\frac{v_nW}{D_n}\right)\exp\left(-\frac{v_nW}{D_n}\right)-1\right]\right\}$$

$$+\frac{v_n+v_p}{v_n}\left(\frac{D_p}{v_pW}\right)\left\{\frac{1}{2}+\left(\frac{D_p}{v_pW}\right)^2\left[\left(1+\frac{v_pW}{D_p}\right)\exp\left(-\frac{v_p}{D_p}W\right)-1\right]\right\}. \qquad (16)$$

To find the expression for $\eta = s_3/\kappa W$, we must now calculate s_3 (see Appendix B). The complete expression for s_3 including diffusion terms is very lengthy. For simplicity, we shall follow Kuvås [4] and calculate s_3 assuming zero diffusion. As mentioned by Kuvås [4], the effect of the term involving η in the differential equation is usually small, and furthermore, there is reason to suspect that higher-order corrections (i.e., corrections due to non-zero carrier transit time) will contribute significantly to η. Thus there is little reason to worry about the small diffusion correction. Under these conditions, our expression for η is as follows:

$$\eta=\frac{(\alpha_n'-\alpha_p')\left(\frac{1}{v_p}+\frac{1}{v_n}\right)}{\kappa W\left(1-e^{-zW}\right)}\left\{\frac{v_nze^{-zW}}{1-e^{-zW}}\left[\frac{2\left(1-e^{-zW}\right)}{z^3W}-\frac{We^{-zW}}{1-e^{-zW}}\left(\frac{1}{z}-\frac{W}{2}\right)-\frac{1}{z^2}\right]\right.$$

$$+\frac{v_p z}{1-e^{-zW}}\left[\frac{2\left(1-e^{-zW}\right)}{z^3 W}-\frac{We^{-zW}}{1-e^{-zW}}\left(\frac{e^{-zW}}{z}+\frac{W}{2}\right)-\frac{We^{-zW}}{z}-\frac{e^{-zW}}{z^2}\right]$$

$$+\left(\alpha_n v_p+\alpha_p v_n\right)\left[\frac{W^2 e^{-zW}}{\left(1-e^{-zW}\right)^2}\left(1+e^{-zW}\right)-\frac{2\left(1-e^{-zW}\right)}{z^3 W}\right]\Bigg\}. \qquad (17)$$

The primes denote differentiation with respect to the electric field (see Table I). For the case of equal ionization rates, it turns out that

$$\eta\big|_{\alpha_n=\alpha_p} \equiv 0 \ . \qquad (18)$$

Although we did not show it explicitly, the expressions given in (6), (7), (11), (13), (14), and (17) are functions of the avalanche region variational voltage V_a. This arises because α_p and α_n, and hence z, are functions of the electric field, which is a function of V_a by (4).

Once the material parameters are specified, the functions $M\tau$, κ, and η are parameterized by W. Also, the function τ is parameterized by W and $r \triangleq I_{ns}/I_{ps}$. Hence, for a given material one could build up a library of these curves, parameterized by W and r. Note that in order to completely specify the circuit model for the PIN avalanche region, the parameters A and I_s are also needed. The evaluation of model parameters is discussed in Section V.

The expressions given above, which were derived for the PIN case at low current density, should be approximately correct for other doping profiles if the parameter W is properly chosen. This is discussed further in Section V.

The static field E_c is determined by W as follows. From (11), the static multiplication factor for the case of equal ionization rates is $\left(1-W\alpha(E_c)\right)^{-1}$, thus

$$1 - W\alpha(E_c) = I_s/I_0 \ . \qquad (19)$$

For all practical purposes this may be replaced by the condition that the multiplication factor goes to infinity, i.e.,

$$1 - W\alpha(E_c) = 0 \ . \qquad (20)$$

For the case of unequal ionization rates, the condition for an infinite multiplication factor is seen from (7) to be

$$\alpha_n(E_c) - \alpha_p(E_c)\exp\left[\left(\alpha_n(E_c) - \alpha_p(E_c)\right)W\right] = 0 \quad . \tag{21}$$

We shall now present a numerical example. The material is assumed to be silicon with the following parameter values:

$$v_n = v_p = 10^7 \frac{cm}{sec},\ D_n = 39 \frac{cm^2}{sec},\ D_p = 16 \frac{cm^2}{sec} \quad .$$

The ionization rate functions are as follows [9]:

$$\alpha_n(E) = 3.8\cdot10^6 \exp\left(-\frac{1.75\cdot10^6}{|E|}\right),\ \alpha_p(E) = 2.25\cdot10^7 \exp\left(-\frac{3.26\cdot10^6}{|E|}\right)$$

here E is in volts/cm and α_n and α_p are in $(cm)^{-1}$. We shall also assume that

$$r = 1 \text{ (i.e., } I_{ns}=I_{ps}=\frac{1}{2}I_s),\quad W = 6.9\cdot10^{-5} \text{ cm.}$$

This value of W gives a critical field of $E_c = 3.76\cdot10^5 \frac{v}{cm}$. The static voltage across the avalanche region is $WE_c \approx 26$ volts. Recall that our analysis is based on the assumption of saturated carrier velocities. This requires a minimum electric field of about $3\cdot10^4$ volts/cm. Thus our equations remain valid for a negative voltage perturbation of approximately -24 volts.

In Figs. 4 and 5 we have plotted the expressions for this example for a range of V_a from -16 to +16 volts. Note that with the assumed low-field values for the diffusion constants, the diffusion correction to κ is small, around 10%.

IV. A DERIVATION OF THE DRIFT REGION MODEL

In this section we derive and discuss our drift region model. Recall from assumption (d) that the carrier velocities are assumed to be saturated. This implies that the diode remains "punched through" for the entire RF cycle.

Consider a p-type drift region extending from x=0 to $x=W_d$, with holes injected from the avalanche region at x=0. Note that in a p-type drift region the electron current is spatially and temporally constant with value I_{ns}. Thus the total particle current is $I_D(x,t) = I_p(x,t) + I_{ns}$, where $I_p(x,t)$ is the hole current. The current continuity equation is

$$q\frac{\partial p}{\partial t} + \frac{1}{A}\frac{\partial I_p}{\partial x} = 0 \tag{22}$$

and the hole current is given by

$$\frac{1}{A} I_p = qv_p p - qD_p \frac{\partial p}{\partial x} . \tag{23}$$

From (22) we obtain

$$\frac{1}{A} \frac{\partial^2 I_p}{\partial x^2} = - q \frac{\partial^2 p}{\partial x \partial t} , \tag{24}$$

and (23) gives

$$\frac{1}{A} \frac{\partial I_p}{\partial t} = qv_p \frac{\partial p}{\partial t} - qD_p \frac{\partial^2 p}{\partial t \partial x} . \tag{25}$$

Combining (22), (24), and (25), we obtain

$$\frac{\partial^2 I_p}{\partial x^2} - \frac{v_p}{D_p} \frac{\partial I_p}{\partial x} - \frac{1}{D_p} \frac{\partial I_p}{\partial t} = 0 . \tag{26}$$

It can be shown that in an n-type drift region, the electron current I_n satisfies an equation similar to (26) with v_p and D_p replaced by v_n and D_n, respectively.

Now consider the boundary conditions. It is assumed that the injected particle current $I_A(\cdot)$ satisfies $I_A(t) = I_0$ for $t \leq 0$. Thus for $t \leq 0$ the drift region is in a steady state and the boundary conditions are

$$I_p(x,t) = I_0 - I_{ns} \text{ for } t \leq 0, \tag{27}$$

$$I_p(0,t) = I_A(t) - I_{ns} . \tag{28}$$

It is convenient to rewrite (26), (27), and (28) in terms of $I_d(x,t) \triangleq I_D(x,t) - I_0$ and $I_a(t) \triangleq I_A(t) - I_0$. The mathematical problem can then be stated as follows:

$$\frac{\partial^2 I_d}{\partial x^2} - \frac{v}{D} \frac{\partial I_d}{\partial x} - \frac{1}{D} \frac{\partial I_d}{\partial t} = 0 \tag{29}$$

$$I_d(x,t) = 0 \quad \text{for} \quad t \leq 0^+ \tag{30}$$

$$I_d(0^+,t) = I_a(t) \tag{31}$$

where $I_a(\cdot)$ is continuous and $I_a(t) = 0$ for $t \leq 0$. We set $v = v_p$ and $D = D_p$ for a p-type drift region; for an n-type drift region we set $v = v_n$ and $D = D_n$.

To obtain a solution to (29), (30), and (31) we define a function $g : \mathbb{R}^2 \to \mathbb{R}$ as follows:

$$g(x,\lambda) \triangleq 0 \quad \text{for } \lambda \leq 0 \tag{32a}$$

$$\triangleq \frac{x}{2\sqrt{\pi D \lambda^3}} \exp\left[-\frac{(x-v\lambda)^2}{4D\lambda}\right] \quad \text{for } \lambda > 0. \tag{32b}$$

Then the desired solution to the above problem is

$$I_d(x,t) = \int_0^t I_a(t-\lambda)\, g(x,\lambda)\, d\lambda \,. \tag{33}$$

Recall the definition of I_e (see (A-4)):

$$I_e(t) \triangleq \frac{1}{W_d} \int_0^{W_d} I_d(x,t)\, dx. \tag{34}$$

If we substitute (33) into (34) and interchange the order of integration (this can be rigorously justified), we obtain the following result:

$$I_e(t) = \frac{1}{\tau_d} \int_0^t I_a(t-\lambda)\, h(\lambda)\, d\lambda \tag{35}$$

where

$$\tau_d \triangleq W_d/v \tag{36}$$

and where $h(\cdot)$ is given by[1]

$$h(\lambda) \triangleq 0 \quad \text{for } \lambda \leq 0, \tag{37a}$$

$$\triangleq \frac{1}{2}\left[\operatorname{erf}\left(\frac{W_d - v\lambda}{2\sqrt{D\lambda}}\right) + \operatorname{erf}\left(\frac{v}{2\sqrt{D}}\sqrt{\lambda}\right)\right] + \frac{1}{v}\sqrt{\frac{D}{\pi\lambda}}\left[\exp\left(-\frac{v^2}{4D}\lambda\right) - \exp\left(-\frac{(W_d - v\lambda)^2}{4D\lambda}\right)\right]$$

$$\text{for } \lambda > 0. \tag{37b}$$

[1] Recall that $\operatorname{erf}(y) \triangleq \frac{2}{\sqrt{\pi}} \int_0^y e^{-\sigma^2}\, d\sigma$. Note that $\operatorname{erf}(\cdot)$ is an odd function, i.e., $\operatorname{erf}(-y) = -\operatorname{erf}(y)$.

The Laplace transform of (37) is

$$H(s) = \frac{1}{2}\left[\frac{1}{s} - \frac{\exp\left(\frac{W_d v}{2D} - \frac{W_d}{\sqrt{D}}\sqrt{s + \frac{v^2}{4D}}\right)}{\sqrt{s + \frac{v^2}{4D}}\left(\sqrt{s + \frac{v^2}{4D}} - \frac{v}{2\sqrt{D}}\right)} + \frac{\frac{v}{2\sqrt{D}}}{s\sqrt{s + \frac{v^2}{4D}}}\right]$$

$$+ \frac{\frac{\sqrt{D}}{v}}{\sqrt{s + \frac{v^2}{4D}}}\left[1 - \exp\left(\frac{W_d v}{2D} - \frac{W_d}{\sqrt{D}}\sqrt{s + \frac{v^2}{4D}}\right)\right]. \tag{38}$$

It is clear from (38) that $H(\cdot)$ cannot be the impedance of a (linear) lumped network. This justifies our statement in connection with Fig. 3 that the one-port shown there must be a linear <u>distributed</u> network.

Of special interest is the case of zero diffusion. From (37) we have

$$\lim_{D\to 0} h(\lambda) = 1, \qquad 0 < \lambda < \tau_d \tag{39a}$$

$$= 0, \qquad \lambda < 0, \ \lambda > \tau_d \ . \tag{39b}$$

A graph is shown in Fig. 6(a). For this case, the controlled current source I_e becomes

$$\lim_{D\to 0} I_e(t) = \frac{1}{\tau_d}\int_0^{\tau_d} I_a(t-\lambda)\, d\lambda = \frac{1}{\tau_d}\int_{t-\tau_d}^{t} I_a(s)\, ds. \tag{40}$$

In Section VI we shall show how (40) can be realized using controlled sources and a lossless, nondispersive transmission line.

We shall not attempt to provide a circuit model for the drift region in the case of nonzero diffusion. However, we have given two examples of $h(\cdot)$ for the case of nonzero diffusion in Figs. 6(b) and (c). Figure 6(b) shows $h(\cdot)$ for a silicon n-type drift region with length $W_d = 10^{-3}$ cm. This corresponds to an approximate operating frequency of 5 GHz. Figure 6(c) is similar except that $W_d = 10^{-4}$ cm, corresponding to an operating frequency of about 50 GHz. It can be seen that the effects of diffusion are more pronounced in shorter length (higher frequency) drift regions. The fact that diffusion effects in the drift

region can be important at millimeter wave frequencies has been discussed previously in the literature [10,11].

V. THE EVALUATION OF THE MODEL PARAMETERS

In this section we will discuss the evaluation of the model parameters. The parameters I_0 and V_0 were discussed in Section II and will not be considered further. As in all IMPATT circuit models, we have assumed a uniform cross-sectional area A. The proper value to use for A must be obtained or estimated from information supplied by the manufacturer. Once the material is specified and A is known, our model of the avalanche region depends upon the doping profile and three parameters: the width L, $r \triangleq I_{ns}/I_{ps}$, and $I_s \triangleq I_{ns} + I_{ps}$. Similarly, our model of the drift region is characterized by the single parameter W_d.

The total depletion layer capacitance, $C_T = \varepsilon A/(L+W_d)$, can be measured as described by Dunn and Dalley [12]. With A known, this immediately gives $d \triangleq L+W_d$. If one chooses the general model corresponding to an arbitrary doping profile, then the associated doping profile must either be supplied by the manufacturer or obtained by measurement via standard methods such as the capacitance-voltage measurement technique [13]. With this information, one can solve for the static current distribution in the diode and estimate the avalanche width L as described by Schroeder and Haddad [14]. With L known, we then obtain $W_d = d-L$.

The standard method of measuring the reverse saturation current I_s is to measure the diode current when it is biased below breakdown. There does not appear to be any discussion in the literature concerning the measurement of $r \triangleq I_{ns}/I_{ps}$. However, this can be estimated from the standard pn junction theory [9]. Note that only the functions ρ and $I_s/(\kappa\tau)$ require the two parameters I_s and r, and usually these functions have only a small effect on the differential equation describing the nonlinear one-port $\mathcal{N}$.

An approximate but more practical method for utilizing our model is to treat the avalanche region as though it has a PIN doping profile and use the expressions given in Section III. This requires the choice of an "effective value" for the parameter W. Recall that once the parameters I_s and r are fixed (usually, these parameters have only a small effect) the response of the one-port $\mathcal{N}$ is characterized by W for the PIN case. Thus for each value of W the small-signal admittance of our model can be obtained.[2] By comparing these curves with the

[2]Each value of W affects not only the nonlinear one-port $\mathcal{N}$ and the capacitor $C_a = \frac{\varepsilon A}{W}$, but it affects the drift region model also since $W_d = d-W$.

measured small-signal admittance, an effective value of W can be chosen. This is essentially the method used by Schroeder and Haddad [14].

Finally, we note that our model is valid only for the active region of the IMPATT diode. In any actual computer simulation, circuit elements accounting for series resistance and package parasitics must be added.

VI. A FIRST-ORDER NONLINEAR CIRCUIT MODEL

In this section we shall present a first-order nonlinear circuit model. Mathematically, our model is similar to (but not exactly the same as) those given by Quang [1,2] and Gupta [3]. It is based on the following assumptions which are in addition to those given previously: (i) The avalanche region has a PIN doping profile and is biased at a low current density, so that the expressions given in Section III apply; (ii) The ionization rates are the same for holes and electrons, i.e., $\alpha_n = \alpha_p = \alpha$; (iii) Carrier diffusion effects are negligible.

Under the conditions listed above, $\eta(V_a) \equiv 0$ (see (18)) and $\kappa(\cdot)$ and $\tau(\cdot)$ are constants, which we shall denote by κ_e and τ_e, respectively. From (10) and (15) we have

$$\kappa_e \tau_e = \frac{W\left(v_p+v_n\right)}{6v_p v_n} \quad . \tag{41}$$

Hence, the differential equation (3) reduces to

$$\frac{dI_a}{dt} - \mu(v_a)\frac{\left(I_a(t)+I_0\right)}{\kappa_e\tau_e} = \frac{I_s}{\kappa_e\tau_e} \tag{42}$$

where, from (11),

$$\mu(V_a) \triangleq W\,\alpha\left(E_c + \frac{V_a}{W}\right) - 1 \; . \tag{43}$$

Equation (42) is basically the same as Read's [8] equation for the avalanche particle current except for the generalization to unequal carrier drift velocities and the inclusion of the constant κ_e, which is a correction for space-charge effects. We can rewrite (42) as follows:

$$\mu(V_a) = \kappa_e\tau_e \frac{d}{dt}\left[\ln\left(I_a+I_0\right)\right] - \frac{I_s}{I_a+I_0} \; . \tag{44}$$

Expanding $\mu(\cdot)$ in a Taylor series and retaining terms up to the second order, we have

$$\mu(V_a) = \mu(0) + \mu'(0)\, V_a + \frac{\mu''(0)}{2} V_a^2 + \ldots$$

$$= W\alpha(E_c) - 1 + \alpha'(E_c)\, V_a + \frac{\alpha''(E_c)}{2W} V_a^2 + \ldots \qquad (45)$$

Substituting (45) into (44) and recalling that $1 - W\alpha(E_c) = I_s/I_0$ (see (19)), we obtain the following result:

$$V_a = \frac{\kappa_e \tau_e}{\alpha'(E_c)} \frac{d}{dt}\left[\ln\left(I_a+I_0\right)\right] + \frac{I_s}{\alpha'(E_c)}\left[\frac{1}{I_0} - \frac{1}{I_a+I_0}\right] - \frac{\alpha''(E_c)}{2W\alpha'(E_c)} V_a^2 \quad . \qquad (46)$$

The terms on the right-hand side of (46) can be interpreted as follows. Evidently, the first term is the voltage across a nonlinear inductor whose ϕ-i curve is given by

$$\phi(I_a) = \frac{\kappa_e \tau_e}{\alpha'(E_c)} \ln\left(I_a+I_0\right) + \phi_0 \qquad (47)$$

where ϕ_0 is an arbitrary constant. The second term is the voltage across a nonlinear resistor whose v-i curve is given by

$$V_R(I_a) = \frac{I_s}{\alpha'(E_c)}\left[\frac{1}{I_0} - \frac{1}{I_0+I_a}\right] \quad . \qquad (48)$$

Finally, the last term is a nonlinear voltage-controlled voltage source.

Recall that we are ignoring diffusion effects, so the controlled current source I_e is described by (40). The nonlinear circuit model based on (40) and (46) is shown in Fig. 7.

There are two comments to be made concerning Fig. 7. First, the controlled voltage source V_N is included to simulate nonlinearities in the avalanche process which can cause low-frequency instabilities when the IMPATT diode is used as an oscillator. The mechanism by which this occurs was described by Brackett [15]. Also, we have shown how the controlled current source I_e can be realized using controlled sources and a lossless, nondispersive transmission line having a characteristic impedance Z_0 and a delay of $\tau_d/2$. To see that the given circuit does in fact realize I_e, note the current I_1 at the input to the transmission line has a forward component and a reflected component which is totally absorbed in the 2-terminal lumped impedance Z_0, thus

$$I_1(t) = I_a(t) - I_a(t-\tau_d)$$

and therefore[3]

$$V_1 = \frac{1}{C_1}\int_0^t \left[I_a(s)-I_a(s-\tau_d)\right]\, ds$$

$$= \frac{1}{C_1}\int_{t-\tau_d}^{t} I_a(s)\, ds.$$

Hence, it follows that $I_e = \frac{C_1 V_1}{\tau_d}$. The use of transmission lines in the modeling of transit-time devices was suggested by Quang [1,2,16].

Finally, in the small-signal limit our avalanche region model reduces to the circuit shown in Fig. 8(a). In Fig. 8(b) is shown the model of Hulin, Claassen, and Harth [17] which is based on a more exact, nonquasistatic, small-signal analysis. For the case of equal ionization rates, both models are identical except for a parallel negative resistance in Hulin's model which is proportional to the inverse of the dc bias current. Recall, however, that our model was derived assuming a "small" dc bias current. Thus we have shown that our model is consistent with the more exact small-signal model of Hulin.

VII. GENERAL COMMENTS AND SUMMARY

There are several comments that need to be made concerning our model. First, the reader has probably noticed that we have not included a simulation example. This was believed to be unnecessary since our model is based on well-established equations and several of the cited references contain simulation examples. Also, we have not discussed noise models since (small-signal) noise models have been discussed previously in the literature [16,18]. Finally, our model of the drift region is based on the assumption of saturated carrier velocities. This assumption implies that the diode remains "punched through" for the entire RF cycle. Thus our model cannot simulate effects such as the "premature collection mode" described by Kuvås and Schroeder [19].

The main contributions of this paper are as follows. We have shown how the transport equations for an IMPATT diode can be written in such a way as to produce a topologically simple circuit model where each element corresponds to some physical operating mechanism inside the device. Our model of the avalanche region is based on the quasistatic analysis of Kuvås and Lee [4,5,6,7], and

[3] It is assumed that $I_a(t) = 0$ for $t \leq 0$ and that $V_1 = 0$ at $t = 0$.

includes the effects of unequal ionization rates, unequal carrier drift velocities, and carrier diffusion. Also, we have shown how diffusion effects in the drift region can be included in the model. These features have not been available in previous circuit models. Finally, we have given explicit equations (which have not been available previously in the literature) for calculating the nonlinear functions associated with the avalanche region model for arbitrary doping profiles.

ACKNOWLEDGEMENT

The authors would like to thank Dr. Y-L Kuo of Bell Telephone Laboratories for his helpful discussions during the initial phase of this research.

APPENDIX

A. TOPOLOGY OF THE GENERAL CIRCUIT MODEL

In this appendix we derive the topology of the circuit model shown in Fig. 1. Symbols which are not defined here are defined in Table I. Consider first the drift region which extends from $x = 0$ to $x = W_d$. The total current I at each point, which is the sum of the particle current and the displacement current, is independent of x and is given by

$$I(t) = I_D(x,t) + \varepsilon A \frac{\partial E_D(x,t)}{\partial t} . \tag{A-1}$$

If (A-1) is integrated from $x = 0$ to $x = W_d$, we have

$$I(t) = \frac{1}{W_d}\int_0^{W_d} I_D(x,t)dx + \frac{\varepsilon A}{W_d}\frac{d}{dt}\int_0^{W_d} E_D(x,t)dx. \tag{A-2}$$

Observing that the total drift region voltage is $V_D(t) = \int_0^{W_d} E_D(x,t)dx$, (A-2) can be rewritten

$$I(t) = \frac{1}{W_d}\int_0^{W_d} [I_0+I_d(x,t)]dx + C_d\frac{dV_D}{dt} = I_0 + I_e(t) + C_d\frac{dV_d}{dt} \tag{A-3}$$

where $C_d \triangleq \frac{\varepsilon A}{W_d}$, I_0 is the static current, and

$$I_e(t) \triangleq \frac{1}{W_d}\int_0^{W_d} I_d(x,t)dx. \tag{A-4}$$

The analogous equation for the avalanche region is

$$I(t) = I_0 + I_a(t) + C_a\frac{dV_a}{dt} \tag{A-5}$$

where $C_a \triangleq \varepsilon A/L$. Note that we have written (A-3) and (A-5) in terms of the voltages V_d and V_a, which are the variations of the drift region and avalanche region voltages, respectively, from their static values. If we denote the sums of the two static voltages by V_0, then the total terminal voltage is given by

$$V(t) = V_0 + V_a(t) + V_d(t). \tag{A-6}$$

Thus if we take V_d to be the voltage across the controlled current source I_e, then it is clear that (A-3) and (A-5) represent KCL, and (A-6) represents KVL, for the circuit shown in Fig. 1.

B. A DERIVATION OF THE DIFFERENTIAL EQUATION FOR THE NONLINEAR ONE-PORT $\mathcal{N}$

Our first step is to discuss some physical variables and present a differential equation which relates them. For convenience, we shall use the symbol J for current

density, e.g., $J_A = I_A/A$ is the spatially-averaged avalanche region particle current density. We define our coordinate system so that impact ionization occurs only between x = 0 and x = L. Note that this is not the same as the coordinate system used in Appendix A. For $0 \leq x \leq L$, define

$$E_i(x) \triangleq E_c + \frac{q}{\varepsilon}\int_0^x N(x_1)dx_1 \tag{A-7}$$

where E_c is the electric field at x = 0 under static conditions and $N(\cdot)$ is the net doping density. Similarly, define

$$E_{sc}(x,t) \triangleq \frac{q}{\varepsilon}\int_0^x [p(x_1,t)-n(x_1,t)]dx_1 - \frac{q}{\varepsilon L}\int_0^L\int_0^x [p(x_1,t)-n(x_1,t)]dx_1dx. \tag{A-8}$$

Note that E_{sc} satisfies the condition

$$\int_0^L E_{sc}(x,t)dx = 0 \tag{A-9}$$

as can be easily verified by integrating (A-8). Finally, define

$$E_a(t) \triangleq E_v(t) + \frac{q}{\varepsilon L}\int_0^L\int_0^x [p(x_1,t)-n(x_1,t)]dx_1dx \tag{A-10}$$

where $E_v(\cdot)$ is the variation of the electric field at x = 0 from its static value E_c. Evidently, the total electric field E is then

$$E(x,t) = E_i(x) + E_a(t) + E_{sc}(x,t). \tag{A-11}$$

The total voltage across the avalanche region is $V_A(t) = \int_0^L E(x,t)dx$. If we separate V_A into its static part, V_A°, and its variational part, V_a, then it follows from (A-9) and (A-11) that $V_A^\circ = \int_0^L E_i(x)dx$ and

$$V_a(t) = LE_a(t). \tag{A-12}$$

The total current J is independent of x and is given by

$$J(t) = J_p(x,t) + J_n(x,t) + \varepsilon\frac{\partial E_{sc}(x,t)}{\partial t} + \varepsilon\frac{dE_a(t)}{dt}. \tag{A-13}$$

From (A-13) it is clear that the quantity J_A, defined below, is a function of t only:

$$J_A(t) \triangleq J_p(x,t) + J_n(x,t) + \varepsilon\frac{\partial E_{sc}(x,t)}{\partial t}. \tag{A-14}$$

Integrating (A-14) and using (A-9), we obtain

$$J_A(t) = \frac{1}{L}\int_0^L [J_p(x,t)+J_n(x,t)]dx. \tag{A-15}$$

Thus we see that J_A, defined in (A-14), is in fact the spatially-averaged particle current.

For convenience, we define the following multiplication factors and time constants:

$$M_p \triangleq \left[1-\int_0^L \alpha_p \exp\left(\int_0^x (\alpha_n-\alpha_p)dx_1\right)dx\right]^{-1} \tag{A-16}$$

$$M_n \triangleq \left[1-\int_0^L \alpha_n \exp\left(\int_x^L (\alpha_p-\alpha_n)dx_1\right)dx\right]^{-1} \tag{A-17}$$

$$\tau_p \triangleq \frac{1}{v_n+v_p}\int_0^L \exp\left[\int_0^x (\alpha_n-\alpha_p)dx_1\right]dx \tag{A-18}$$

$$\tau_n \triangleq \frac{1}{v_n+v_p}\int_0^L \exp\left[\int_x^L (\alpha_p-\alpha_n)dx_1\right]dx \tag{A-19}$$

$$M \triangleq \frac{1}{J_s}[M_n J_{ns}+M_p J_{ps}] \tag{A-20}$$

$$\tau \triangleq J_s\left[\frac{J_{ns}}{\tau_n}+\frac{J_{ps}}{\tau_p}\right]^{-1}. \tag{A-21}$$

The following relationships can be shown in a straightforward manner:

$$\frac{M_n}{M_p} = \frac{\tau_p}{\tau_n} = \exp\left[\int_0^L (\alpha_n-\alpha_p)dx\right] \tag{A-22}$$

$$M_n\tau_n = M_p\tau_p = M\tau. \tag{A-23}$$

We shall assume that holes are traveling in the positive x direction. It follows that the boundary conditions for J_p and J_n are

$$J_p(0,t) = J_{ps} \tag{A-24}$$

$$J_n(L,t) = J_{ns}. \tag{A-25}$$

Under these conditions, Kuvås [4] has derived the following differential equation:[4]

[4] We have corrected the third term on the right-hand side of (A-26). Kuvås [4] shows a factor of $(\alpha_n v_n+\alpha_p v_p)$, or in his notation, $(\alpha v_n+\beta v_p)$. This term was given correctly in a paper by Kuvås and Lee [5], although this paper ignored diffusion effects.

$$\frac{dJ_A}{dt} + \frac{J_A(t)}{M\tau} - \frac{J_s}{\tau} = \frac{v_n}{(v_n+v_p)\tau_p}\varepsilon\frac{\partial E_{sc}(0,t)}{\partial t} + \frac{v_p}{(v_n+v_p)\tau_n}\varepsilon\frac{\partial E_{sc}(L,t)}{\partial t}$$

$$- \frac{1}{(v_n+v_p)\tau_n}\int_0^L\left[(\alpha_n v_p+\alpha_p v_n)\varepsilon\frac{\partial E_{sc}}{\partial t} - \varepsilon\frac{\partial^2 E_{sc}}{\partial t^2}\right]\exp\left[\int_x^L(\alpha_p-\alpha_n)dx_1\right]dx$$

$$+ \frac{q}{(v_n+v_p)\tau_n}\int_0^L\left[D_n\frac{\partial^2 n}{\partial t\partial x} - D_p\frac{\partial^2 p}{\partial t\partial x}\right]\exp\left[\int_x^L(\alpha_p-\alpha_n)dx_1\right]dx. \qquad \text{(A-26)}$$

Recall from (A-8) that E_{sc} is a functional of p and n. Thus all the "correction terms" on the right-hand side of (A-26) require a solution for p and n. If we assume that the time variations are "slow" enough (compared to the carrier transit time across the avalanche region), then we may use the following quasistatic approximations for p and n:

$$qp^\circ(x,t) = \frac{J_A(t)-J_{ns}}{v_p}\exp\left[\frac{v_p}{D_p}(x-L)\right] + \frac{1}{D_p}\int_x^L J_p^\circ(x_1,t)\exp\left[\frac{v_p}{D_p}(x-x_1)\right]dx_1 \qquad \text{(A-27)}$$

$$qn^\circ(x,t) = \frac{J_A(t)}{v_n} - \frac{J_{ps}}{v_n}\exp\left(\frac{-v_n}{D_n}x\right) - \frac{1}{D_n}\int_0^x J_p^\circ(x_1,t)\exp\left[\frac{v_n}{D_n}(x_1-x)\right]dx_1 \qquad \text{(A-28)}$$

where

$$J_p^\circ(x,t) = J_{ps}\exp\left[\int_0^x(\alpha_p-\alpha_n)dx_1\right] + \left[J_A(t)-J_{ns}-J_{ps}\exp\left(\int_0^L(\alpha_p-\alpha_n)dx\right)\right]$$
$$\cdot\frac{\int_0^x\alpha_n\exp\left[\int_{x_1}^x(\alpha_p-\alpha_n)dx_2\right]dx_1}{\int_0^L\alpha_n\exp\left[\int_x^L(\alpha_p-\alpha_n)dx_1\right]dx}. \qquad \text{(A-29)}$$

The superscript zero signifies a static approximation for a dynamic variable. Here the time dependence of J_p° arises both from $J_A(t)$ and the fact that α_p and α_n are functions of the time-dependent electric field. The approximate electric field used in evaluating all ionization integrals is

$$E^\circ(x,t) = E_i(x) + E_a(t) + E_s(x) \qquad \text{(A-30)}$$

where $E_s(x)$ is some sort of low-order correction for the space-charge field $E_{sc}(x,t)$ (compare with (A-11)). Usually, we assume that the current density is small enough so that E_s may be ignored.

If we use the quasistatic carrier densities given in (A-27) and (A-28) to

evaluate the correction terms on the right-hand side of (A-26) and if we ignore the second-order time derivative (this is consistent with the assumption of "slow" time variations) then after some straightforward calculations it is found that (A-26) can be written in the form

$$\frac{dJ_A}{dt} + \frac{J_A(t)}{M(E_a)\tau(E_a)} = \frac{J_s}{\tau(E_a)} + s_1(E_a)\frac{dJ_A}{dt} + s_2(E_a)\frac{dE_a}{dt} + s_3(E_a)J_A(t)\frac{dE_a}{dt} \,. \qquad \text{(A-31)}$$

We shall give expressions for s_1, s_2, and s_3. First, however, we must make the following definitions:

$$f_1(x,E_a) \triangleq \frac{\int_0^x \alpha_n \exp\left[\int_{x_1}^x (\alpha_p-\alpha_n)dx_2\right]dx_1}{\int_0^L \alpha_n \exp\left[\int_x^L (\alpha_p-\alpha_n)dx_1\right]dx} \qquad \text{(A-32)}$$

$$\begin{aligned} f_2(x,E_a) \triangleq\ & J_{ps}\exp\left[\int_0^x (\alpha_p-\alpha_n)dx\right]\int_0^x (\alpha_p'-\alpha_n')dx_1 - \frac{1}{\int_0^L \alpha_n \exp\left[\int_x^L (\alpha_p-\alpha_n)dx_1\right]dx} \\ & \cdot\left\{J_{ps}\exp\left(\int_0^L (\alpha_p-\alpha_n)dx\right)\cdot\int_0^L (\alpha_p'-\alpha_n')dx \int_0^x \alpha_n \exp\left[\int_{x_1}^x (\alpha_p-\alpha_n)dx_2\right]dx_1\right. \\ & + \left[J_{ns}+J_{ps}\exp\left(\int_0^L (\alpha_p-\alpha_n)dx\right)\right]\cdot\int_0^x\left[\alpha_n'+\alpha_n\int_{x_1}^x (\alpha_p'-\alpha_n')dx_2\right] \\ & \left.\cdot\exp\left[\int_{x_1}^x (\alpha_p-\alpha_n)dx_2\right]dx_1\right\} + \frac{\int_0^x \alpha_n \exp\left[\int_{x_1}^x (\alpha_p-\alpha_n)dx_2\right]dx_1}{\left[\int_0^L \alpha_n \exp\left(\int_x^L (\alpha_p-\alpha_n)dx_1\right)dx\right]^2} \\ & \cdot\left[J_{ns}+J_{ps}\exp\left(\int_0^L (\alpha_p-\alpha_n)dx\right)\right]\int_0^L\left[\alpha_n'+\alpha_n\int_x^L (\alpha_p'-\alpha_n')dx_1\right] \\ & \cdot\exp\left[\int_x^L (\alpha_p-\alpha_n)dx_1\right]dx \end{aligned} \qquad \text{(A-33)}$$

$$f_3(x,E_a) \triangleq \frac{\int_0^x \left[\alpha_n' + \alpha_n \int_{x_1}^x (\alpha_p' - \alpha_n')dx_2\right] \exp\left[\int_{x_1}^x (\alpha_p - \alpha_n)dx_2\right] dx_1}{\int_0^L \alpha_n \exp\left[\int_x^L (\alpha_p - \alpha_n)dx_1\right] dx}$$

$$- \frac{\int_0^x \alpha_n \exp\left[\int_{x_1}^x (\alpha_p - \alpha_n)dx_2\right] dx_1}{\left[\int_0^L \alpha_n \exp\left(\int_x^L (\alpha_p - \alpha_n)dx_1\right) dx\right]^2} \cdot \int_0^L \left[\alpha_n' + \alpha_n \int_x^L (\alpha_p' - \alpha_n')dx_1\right]$$

$$\cdot \exp\left[\int_x^L (\alpha_p - \alpha_n)dx_1\right] dx. \qquad \text{(A-34)}$$

For convenience, we define the following function $\delta(\cdot)$:

$$\delta(1) \triangleq 1 \qquad \text{(A-35a)}$$

$$\delta(2) \triangleq \delta(3) \triangleq 0. \qquad \text{(A-35b)}$$

Next, we define

$$r_i(x,E_a) \triangleq -\delta(i)\exp\left[\frac{v_p}{D_p}(x-L)\right] + \frac{v_n}{D_n}\int_0^x f_i(x_1,E_a)\exp\left[\frac{v_n}{D_n}(x_1-x)\right]dx_1$$

$$- \frac{v_p}{D_p}\int_x^L f_i(x_1,E_a)\exp\left[\frac{v_p}{D_p}(x-x_1)\right]dx_1 \qquad \text{for } i = 1,2,3; \qquad \text{(A-36)}$$

and

$$h_i(x,E_a) \triangleq \delta(i)\left\{\frac{D_p}{v_p^2}\exp\left[\frac{v_p}{D_p}(x-L)\right] - \frac{D_p^2}{v_p^3 L}\left[1-\exp\left(\frac{-v_p}{D_p}L\right)\right] + \frac{1}{v_n}\left(\frac{1}{2}L-x\right)\right\}$$

$$+ \left(\frac{1}{v_n}+\frac{1}{v_p}\right)\left[\int_0^x f_i(x_1,E_a)dx_1 - \frac{1}{L}\int_0^L (L-x)f_i(x,E_a)dx\right]$$

$$- \frac{1}{v_n}\int_0^x \exp\left(\frac{v_n}{D_n}(x_1-x)\right) f_i(x_1,E_a)dx_1 + \frac{1}{v_p}\int_x^L \exp\left(\frac{v_p}{D_p}(x-x_1)\right) f_i(x_1,E_a)dx_1$$

$$+ \frac{D_n}{v_n^2 L}\int_0^L \left[1-\exp\left(\frac{v_n}{D_n}(x-L)\right)\right] f_i(x,E_a)dx$$

$$+ \frac{D_p}{v_p^2 L}\int_0^L \left[\exp\left(\frac{-v_p}{D_p}x\right)-1\right] f_i(x,E_a)dx \qquad \text{for } i = 1,2,3. \qquad \text{(A-37)}$$

Finally, s_1, s_2, and s_3 are given by

$$s_i(E_a) \triangleq \frac{v_n}{(v_n+v_p)\tau_p(E_a)} h_i(0,E_a) + \frac{v_p}{(v_n+v_p)\tau_n(E_a)} h_i(L,E_a)$$

$$-\frac{1}{(v_n+v_p)\tau_n(E_a)} \int_0^L (\alpha_n v_p + \alpha_p v_n) h_i(x,E_a) \exp\left[\int_x^L (\alpha_p-\alpha_n)dx_1\right]dx$$

$$+\frac{1}{(v_n+v_p)\tau_n(E_a)} \int_0^L r_i(x,E_a) \exp\left[\int_x^L (\alpha_p-\alpha_n)dx_1\right]dx, \qquad \text{for } i = 1,2,3. \tag{A-38}$$

The functions M and τ can be expressed equally well in terms of $V_a = LE_a$ (see (A-12)). By a slight abuse of notation, we shall denote these quantities by $M(V_a)$ and $\tau(V_a)$. Equation (A-31) can then be rewritten in terms of V_a and $I_A = AJ_A$ as follows:

$$\frac{dI_A}{dt} + \frac{I_A(t)}{M(V_a)\kappa(V_a)\tau(V_a)} = \frac{I_s}{\kappa(V_a)\tau(V_a)} + \eta(V_a)(I_A - \rho(V_a)I_s)\frac{dV_a}{dt} \tag{A-39}$$

where

$$\kappa(V_a) \triangleq 1 - s_1\left(\frac{V_a}{L}\right) \tag{A-40}$$

$$\eta(V_a) \triangleq \frac{1}{L\kappa(V_a)} s_3\left(\frac{V_a}{L}\right) \tag{A-41}$$

$$\rho(V_a) \triangleq \frac{-s_2\left(\frac{V_a}{L}\right)}{J_s s_3\left(\frac{V_a}{L}\right)} . \tag{A-42}$$

Finally, we should note that Kuvås [4] and Kuvås and Lee [5] have shown that the precise choice of the avalanche zone boundaries (0 and L) is not critical as long as all significant impact ionization is included between these boundaries and L is small enough to justify the quasistatic approximation.

REFERENCES

[1] N. Quang A, "On the Modelling of IMPATT Diodes," in Annual of the Research Institute for Telecommunication 1975, Budapest, Hungary, pp. 155-166, 1975.

[2] N. Quang A, "A Lumped-Distributed Large-Signal Equivalent Circuit for IMPATT Diodes," private communication.

[3] M. S. Gupta, "A Nonlinear Equivalent Circuit for IMPATT Diodes," Solid-State Electronics, vol. 19, pp. 23-26, Jan. 1976.

[4] R. L. Kuvås, "Nonlinear Study of Semiconductor Avalanches," Ph.D. Thesis, Cornell Univ., Ithaca, N.Y., Sept. 1970.

[5] R. Kuvås and C. A. Lee, "Quasistatic Approximation for Semiconductor Avalanches," Journal of Applied Physics, vol. 41, pp. 1743-1755, March 1970.

[6] R. Kuvås and C. A. Lee, "Nonlinear Analysis of Multifrequency Operation of Read Diodes," Ibid., pp. 1756-1767.

[7] R. Kuvås and C. A. Lee, "Carrier Diffusion in Semiconductor Avalanches," Journal of Applied Physics, vol. 41, pp. 3108-3116, June 1970.

[8] W. T. Read, "A Proposed High-Frequency, Negative Resistance Diode," The Bell System Tech. Journal, vol. 37, pp. 401-446, March 1958.

[9] S. M. Sze, Physics of Semiconductor Devices, New York: Wiley, 1969.

[10] B. Culshaw, "Effect of Carrier Diffusion on Operation of Avalanche Diodes," Electronics Letters, vol. 10, pp. 143-145, May 1974.

[11] M. Ohmori, "Optimum Transit Angles of Millimeter-Wave Si IMPATT Diodes," IEEE Trans. on Electron Devices, vol. ED-22, pp. 363-365, June 1975.

[12] C. N. Dunn and J. E. Dalley, "Computer-Aided Small-Signal Characterization of IMPATT Diodes," IEEE Trans. on Microwave Theory and Tech., vol. MTT-17, pp. 691-695, Sept. 1969.

[13] J. Hilibrand and R. D. Gold, "Determination of the Impurity Distribution in Junction Diodes from Capacitance-Voltage Measurements," RCA Review, vol. 21, pp. 245-252, June 1960.

[14] W. E. Schroeder and G. I. Haddad, "Nonlinear Properties of IMPATT Devices," Proceedings of the IEEE, vol. 61, pp. 153-182, Feb. 1973.

[15] C. A. Brackett, "The Elimination of Tuning-Induced Burnout and Bias-Circuit Oscillations in IMPATT Oscillators," The Bell System Tech. Journal, vol. 52, pp. 271-306, March 1973.

[16] N. Quang A, "A Lumped-Distributed Small-Signal Model for a Class of Transit-Time Semiconductor Devices," Int. Journal of Circuit Theory and Applications,

vol. 4, pp. 357-370, Oct. 1976.

[17] R. Hulin, M. Claassen, and W. Harth, "Circuit Representation of Avalanche Region of IMPATT Diodes for Different Carrier Velocities and Ionisation Rates of Electrons and Holes," Electronics Letters, vol. 6, pp. 849-850, Dec. 1970.

[18] M. S. Gupta, "A Small-Signal and Noise Equivalent Circuit for IMPATT Diodes," IEEE Trans. on Microwave Theory and Tech., vol. MTT-21, pp. 591-594, Sept. 1973.

[19] R. L. Kuvås and W. E. Schroeder, "Premature Collection Mode in IMPATT Diodes," IEEE Trans. on Electron Devices, vol. ED-22, pp. 549-558, Aug. 1975.

FIGURE CAPTIONS

Fig. 1. The general circuit model for an SDR IMPATT diode. The function $h(\cdot)$ is given in (2), and $\tau_d \triangleq W_d/v$, where v is the velocity of the majority carriers in the drift region. A derivation of the circuit model's structure is given in Appendix A. See Sections III and IV for other details.

Fig. 2. (a) Circuit model of the avalanche region utilizing a linear inductor and a nonlinear controlled voltage source.

(b) Circuit model equivalent to (a) which utilizes a nonlinear inductor. The constants b and ϕ_0 are arbitrary.

Fig. 3. An illustration showing how the controlled current source I_e can be modeled using a linear, distributed one-port with current impulse response $h(\cdot)$.

Fig. 4. The functions κ_{dr}, κ_{diff}, and κ for a silicon PIN avalanche region of width $W = 6.9\text{x}10^{-5}$cm.

(a) κ_{dr} vs. V_a.

(b) κ_{diff} vs. V_a.

(c) $\kappa = \kappa_{dr} + \kappa_{diff}$ vs. V_a.

Fig. 5. The various nonlinear functions associated with (3) for a silicon PIN avalanche region of width $W = 6.9\text{x}10^{-5}$cm. Recall from (5) that $\rho(V_a) \equiv 1$ in this case.

(a) $(\kappa\tau)^{-1}$ vs. V_a, assuming $r = 1$.

(b) η vs. V_a.

(c) $(M\kappa\tau)^{-1}$ vs. V_a.

Fig. 6. Graphs of the function $h(\cdot)$ given in (37).

(a) $h(\cdot)$ in the limit of no diffusion.

(b) $h(\cdot)$ for a silicon n-type drift region of length $W_d = 10^{-3}$cm. Here $v_n = 10^7$cm/sec, $D_n = 39$ cm^2/sec, and $\tau_d = W_d/v_n = 10^{-10}$sec.

(c) Similar to (b) with $W_d = 10^{-4}$cm and $\tau_d = 10^{-11}$sec.

Fig. 7. A first-order nonlinear circuit model for an SDR IMPATT diode. $\kappa_e\tau_e = W(v_p+v_n)/(6v_pv_n)$ and $\tau_d = W_d/v$, where v is the velocity of the majority carriers in the drift region. In the upper right is shown an open-circuited transmission line of impedance Z_0 and delay $\tau_d/2$. The impedance Z_0 and the capacitance C_1 can be any convenient values.

Fig. 8. (a) The small-signal model of the avalanche region based on Fig. 7. Here

$$C_a = \varepsilon A/W,\ R_{I_s} = \frac{I_s}{I_0^2\alpha'(E_c)},\ \text{and}\ L_a = \frac{\kappa_e\tau_e}{\alpha'(E_c)I_0} = \frac{W(\frac{1}{v_n}+\frac{1}{v_p})}{6\alpha'(E_c)I_0}.$$

(b) The small-signal avalanche region model of Hulin, Claassen, and Harth [17]. For equal ionization rates, all elements have the same values as in (a). In addition,

$$R_a = \left(\frac{1}{\gamma}\right) \frac{5}{\alpha'(E_c) I_0} ,$$

where γ is a constant near unity.

TABLE I. LIST OF SYMBOLS

A	cross-sectional area
D	diffusion constant
E	electric field in the avalanche region
$E_a = V_a/L$	(see V_a and L below)
E_c	static electric field in a PIN avalanche region
E_D	electric field in the drift region
I	terminal current
I_A	spatially-averaged particle current in the avalanche region
$I_a \triangleq I_A - I_0$	(see I_0 below)
I_D	drift region particle current
$I_d \triangleq I_D - I_0$	(see I_0 below)
I_0	terminal current under static conditions
I_{ns}	electron current incident on the avalanche region
I_{ps}	hole current incident on the avalanche region
$I_s \triangleq I_{ns} + I_{ps}$	
L	width of the avalanche region
q	electronic charge
$r \triangleq I_{ns}/I_{ps}$	
v	carrier velocity
V	terminal voltage
V_a	variation of the avalanche region voltage from its static value
V_d	variation of the drift region voltage from its static value
V_0	terminal voltage under static conditions
W	width of a PIN avalanche region
W_d	width of the drift region
$z \triangleq \alpha_n - \alpha_p$	
α	ionization coefficient
$\alpha' \triangleq d\alpha(E)/dE$	
$\alpha'' \triangleq d^2\alpha(E)/dE^2$	
ε	dielectric permittivity of the semiconductor

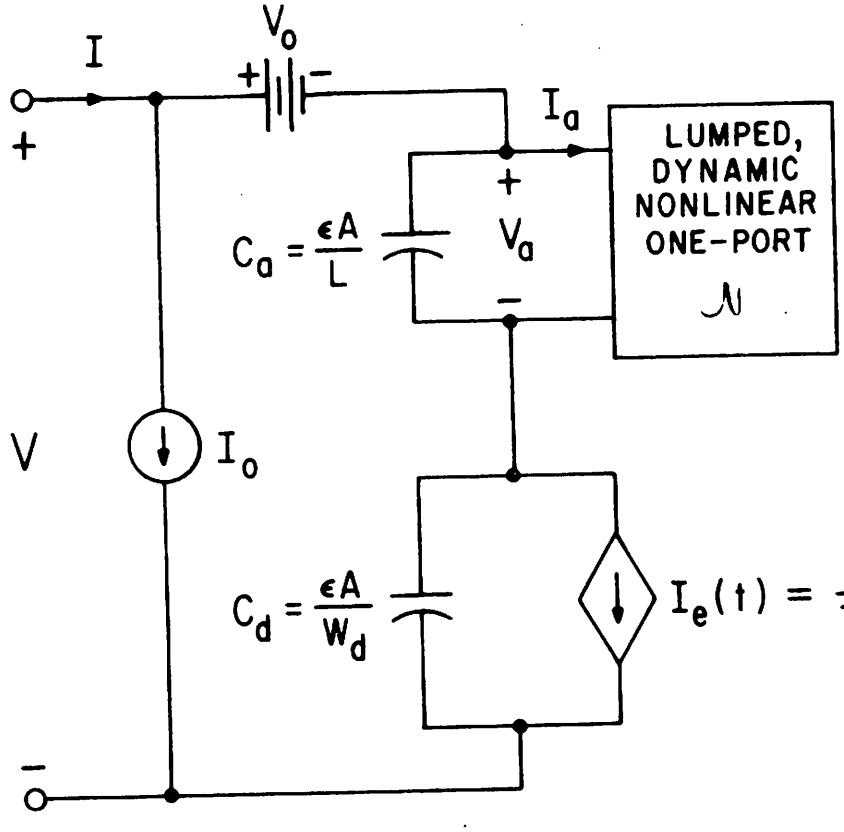

$$\frac{dI_a}{dt} + \frac{I_a + I_o}{M(V_a)\kappa(V_a)\tau(V_a)} =$$

$$\frac{I_s}{\kappa(V_a)\tau(V_a)} + \eta(V_a)\left(I_a + I_o - \rho(V_a) I_s\right) \frac{dV_a}{dt}$$

$$I_e(t) = \frac{1}{\tau_d} \int_0^t I_a(t-\lambda)\, h(\lambda)\, d\lambda$$

Fig. 1

(a)

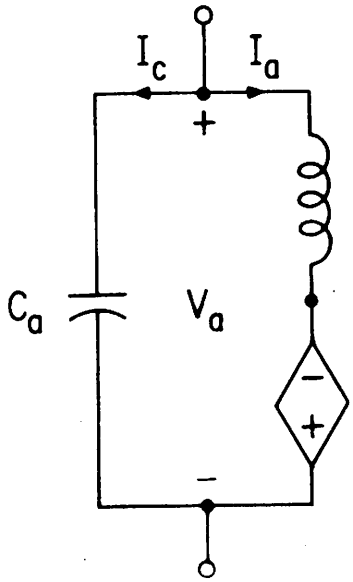

$V_l = f_a(I_a, V_a, I_c)$

$$f_a(I_a,V_a,I_c) \triangleq \frac{-(I_a+I_o)}{M(V_a)\kappa(V_a)\tau(V_a)} - V_a + \frac{I_s}{\kappa(V_a)\tau(V_a)} + \eta(V_a)(I_a+I_o-\rho(V_a)I_s)\frac{I_c}{C_a}$$

(b)

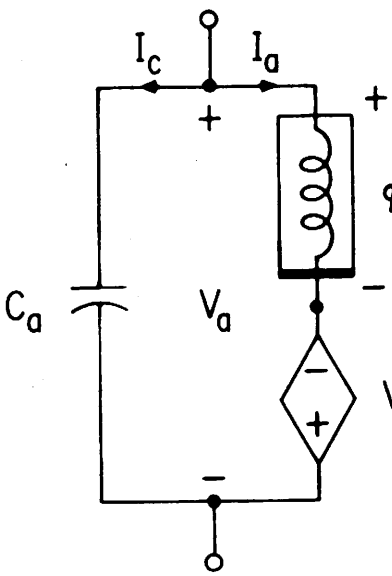

$\phi = \frac{1}{b}\ln(I_a + I_o) + \phi_o$

$V_l = g_a(I_a, V_a, I_c)$

$$g_a(I_a,V_a,I_c) \triangleq \frac{-l}{bM(V_a)\kappa(V_a)\tau(V_a)} - V_a + \frac{I_s}{b(I_a+I_o)\kappa(V_a)\tau(V_a)} + \frac{\eta(V_a)(I_a+I_o-\rho(V_a)I_s)I_c}{b(I_a+I_o)C_a}$$

Fig. 2

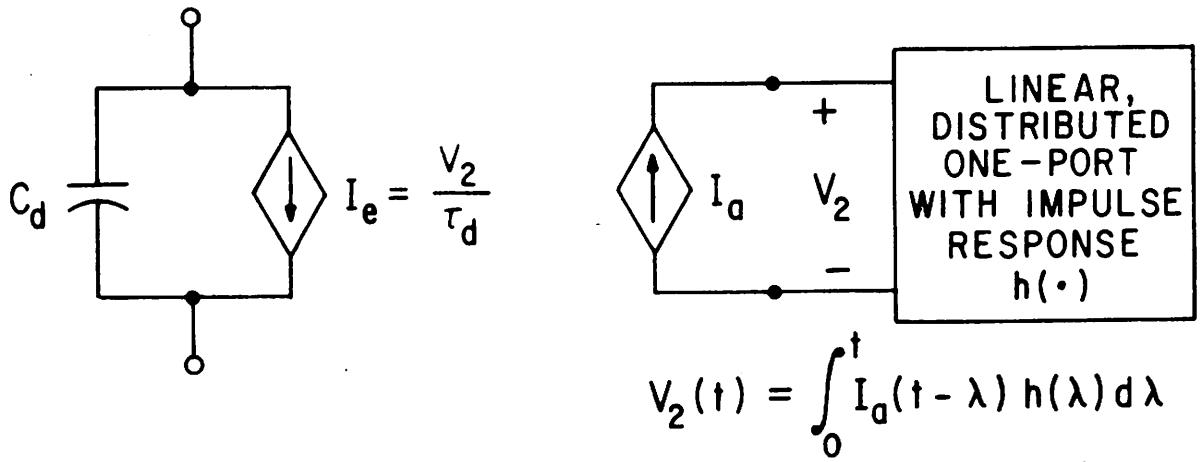
C_d
$I_e = \frac{V_2}{\tau_d}$
I_a
V_2
+
−
LINEAR, DISTRIBUTED ONE-PORT WITH IMPULSE RESPONSE $h(\cdot)$
$V_2(t) = \int_0^t I_a(t-\lambda)\, h(\lambda)\, d\lambda$

Fig. 3

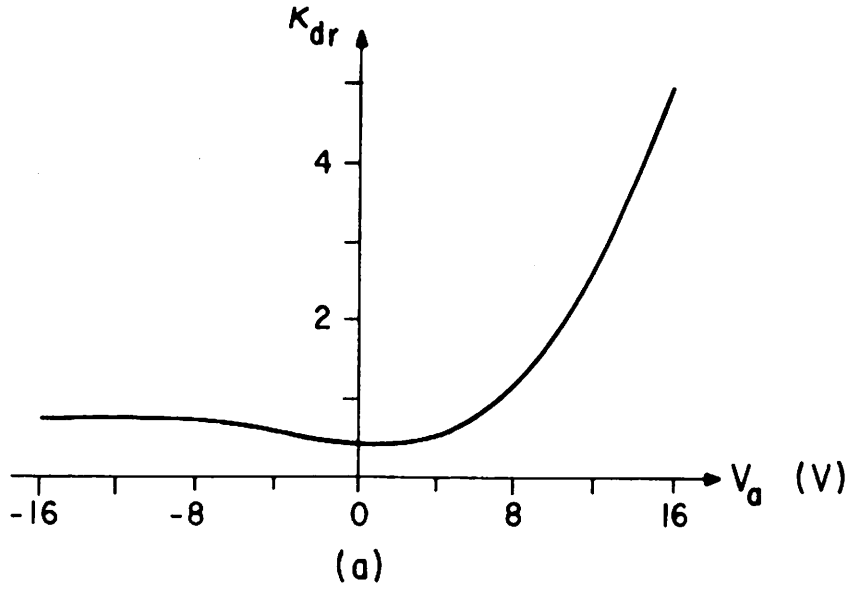
K_{dr}
4
2
V_a (V)
-16
-8
0
8
16

(a)

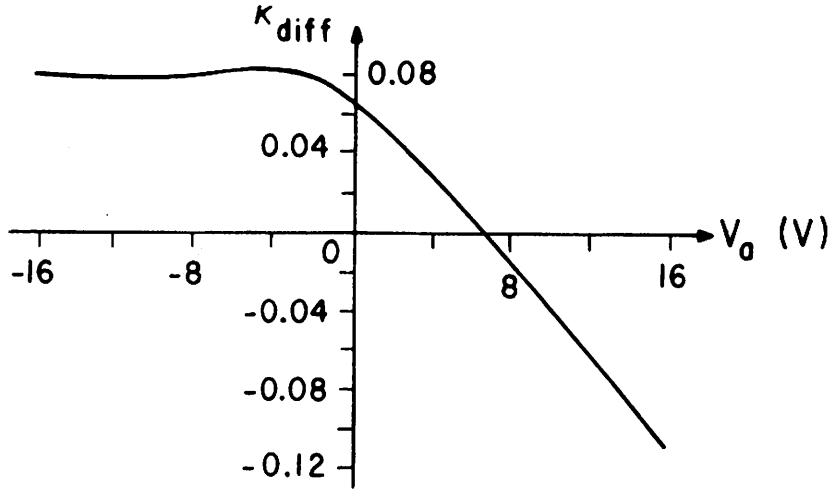
K_{diff}
0.08
0.04
0
-0.04
-0.08
-0.12
V_a (V)
-16
-8
8
16

(b)

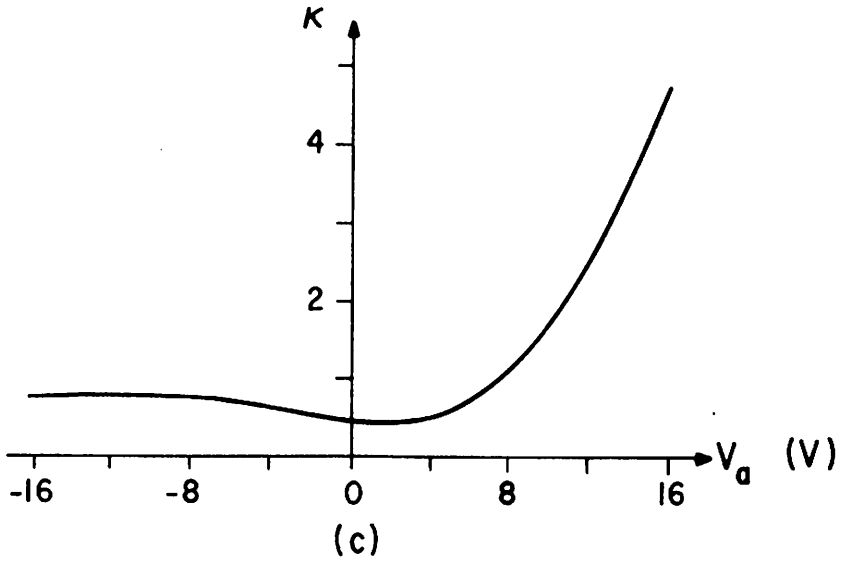
K
4
2
V_a (V)
-16
-8
0
8
16

(c)

Fig. 4

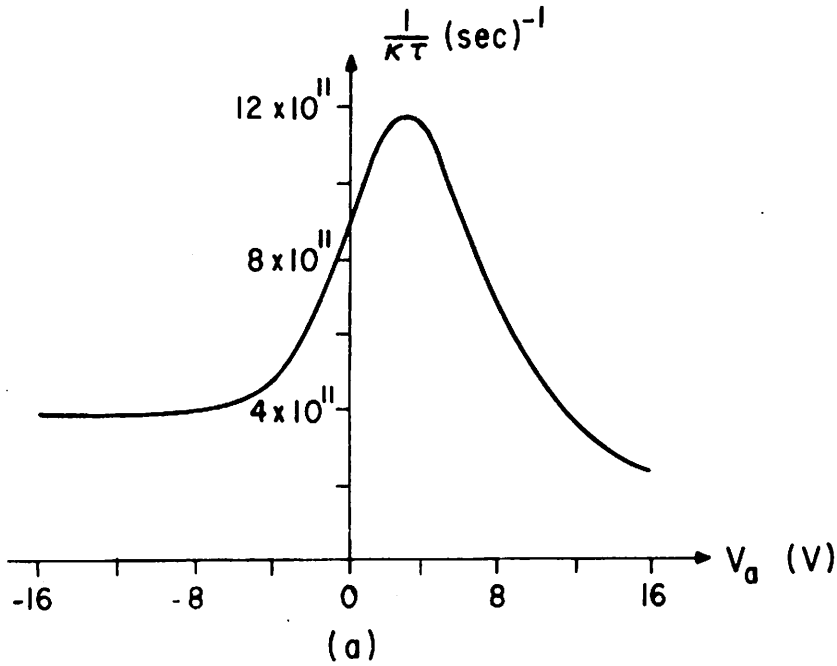
$\frac{1}{\kappa\tau}$ (sec)$^{-1}$
12 x 10^{11}
8 x 10^{11}
4 x 10^{11}
-16
-8
0
8
16
V_a (V)

(a)

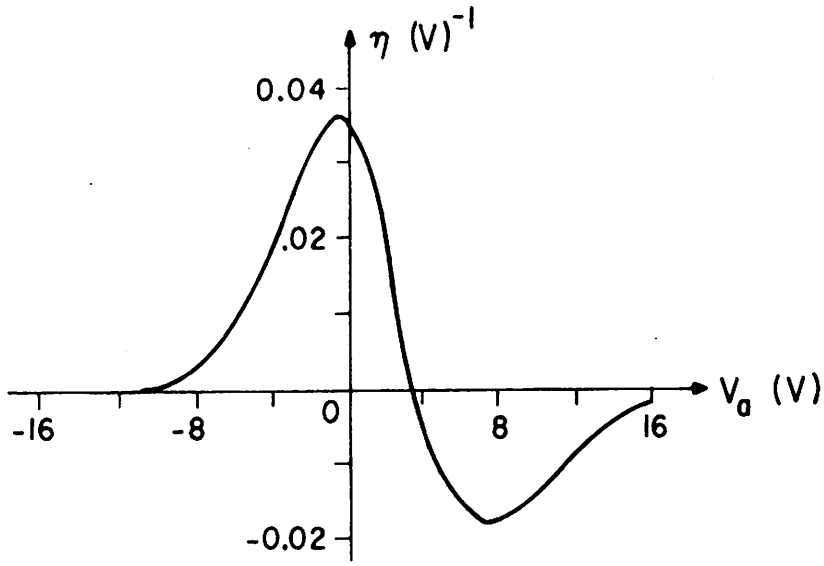
η (V)$^{-1}$
0.04
.02
-0.02
-16
-8
0
8
16
V_a (V)

(b)

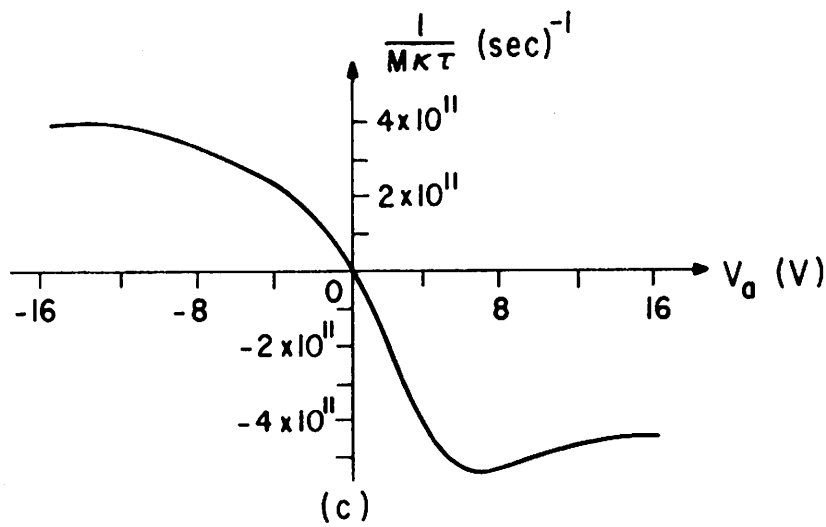
$\frac{1}{M\kappa\tau}$ (sec)$^{-1}$
4x10^{11}
2x10^{11}
-2 x10^{11}
-4 x10^{11}
-16
-8
0
8
16
V_a (V)

(c)

Fig. 5

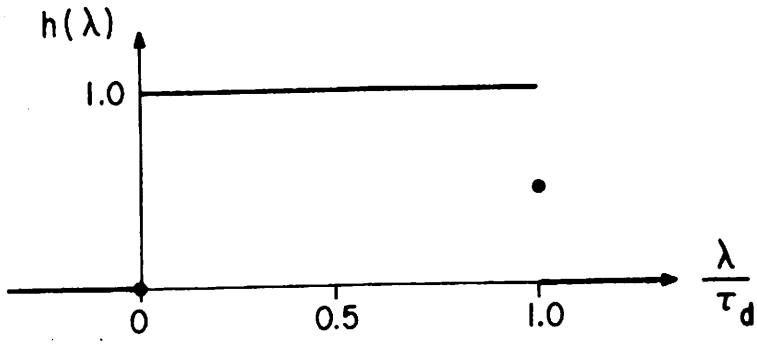

(a)

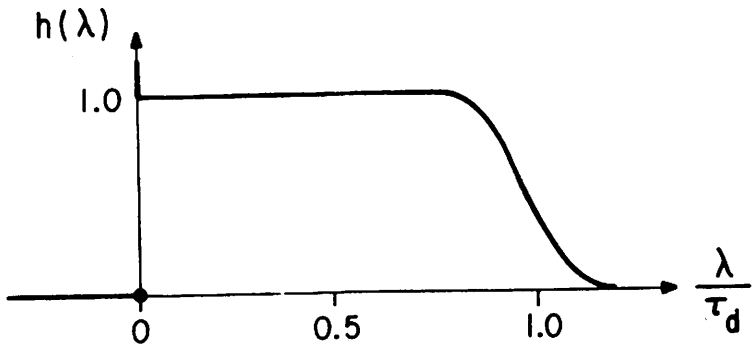

(b)

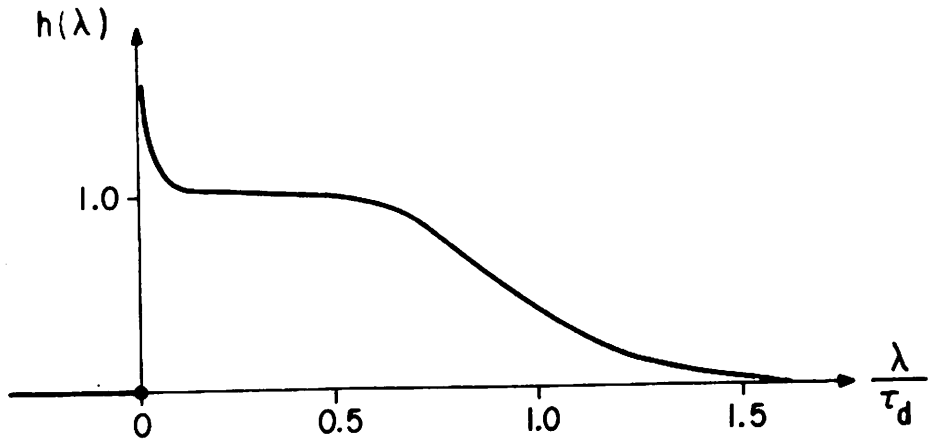

(c)

Fig. 6

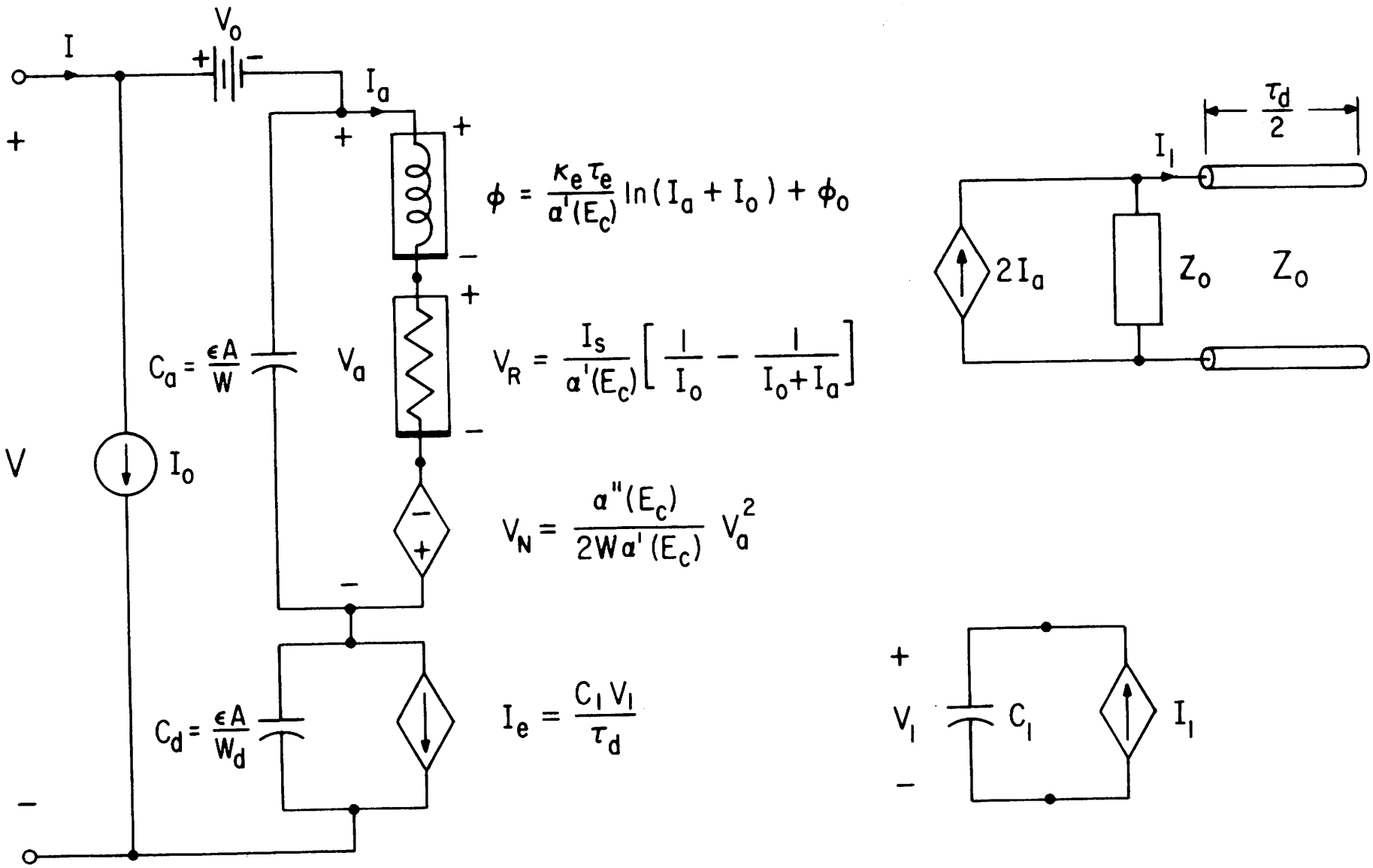
I
V_o
I_a
$\phi = \frac{\kappa_e \tau_e}{\alpha'(E_c)} \ln(I_a + I_o) + \phi_o$
$C_a = \frac{\epsilon A}{W}$
V_a
$V_R = \frac{I_s}{\alpha'(E_c)}\left[\frac{1}{I_o} - \frac{1}{I_o + I_a}\right]$
V
I_o
$V_N = \frac{\alpha''(E_c)}{2W\alpha'(E_c)} V_a^2$
$C_d = \frac{\epsilon A}{W_d}$
$I_e = \frac{C_l V_l}{\tau_d}$
$\frac{\tau_d}{2}$
I_l
$2I_a$
Z_o
Z_o
V_l
C_l
I_l

Fig. 7

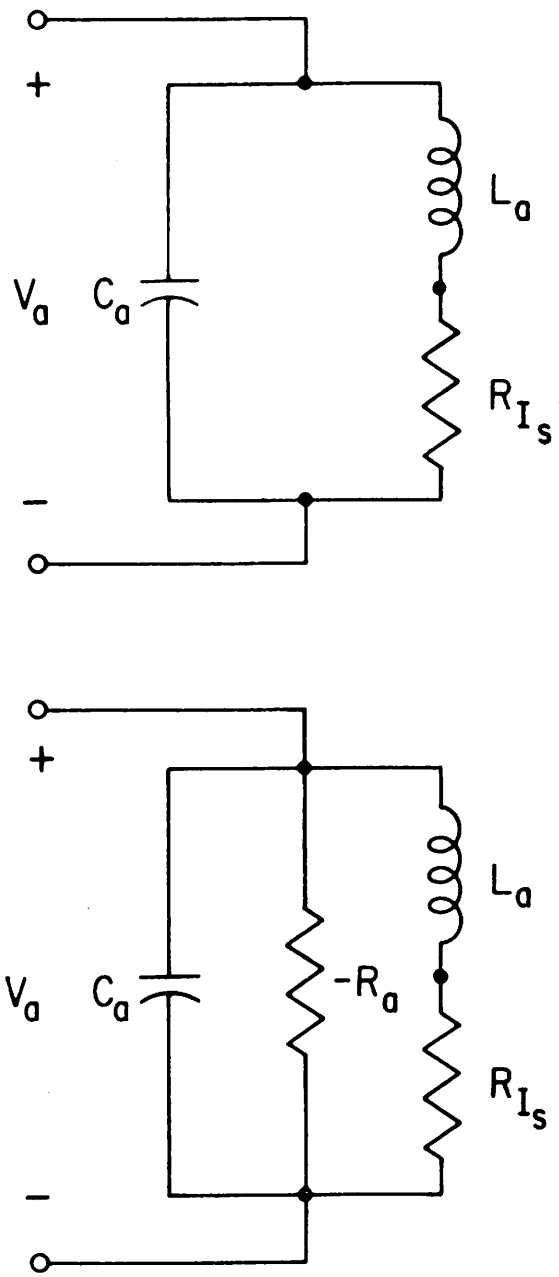

Fig. 8